Journal of
Mechanics of Materials and Structures

A VARIATIONAL ASYMPTOTIC MICROMECHANICS MODEL FOR PREDICTING CONDUCTIVITIES OF COMPOSITE MATERIALS

Tian Tang and Wenbin Yu

Volume 2, Nº 9 *November 2007*

mathematical sciences publishers

JOURNAL OF MECHANICS OF MATERIALS AND STRUCTURES
Vol. 2, No. 9, 2007

A VARIATIONAL ASYMPTOTIC MICROMECHANICS MODEL FOR PREDICTING CONDUCTIVITIES OF COMPOSITE MATERIALS

TIAN TANG AND WENBIN YU

The focus of this paper is to extend the variational asymptotic method for unit cell homogenization (VAMUCH) to predict the effective thermal conductivity and local temperature field distribution of heterogeneous materials. Starting from a variational statement of the conduction problem of the heterogeneous continuum, we formulate the micromechanics model as a constrained minimization problem using the variational asymptotic method. To handle realistic microstructures in applications, we implement this new model using the finite element method. For validation, a few examples are used to demonstrate the application and accuracy of this theory and companion code. Since heat conduction is mathematically analogous to electrostatics, magnetostatics, and diffusion, the present model can also be used to predict effective dielectric, magnetic, and diffusion properties of heterogeneous materials.

1. Introduction

Along with increased knowledge and manufacturing techniques for materials, more and more materials are made with engineered microstructures to achieve better performance. To successfully design and fabricate these materials, we need efficient high-fidelity analysis tools to predict their effective properties. Many composites are applied in temperature sensitive environments such as electronic packaging and thermal protection systems. Accurate prediction of thermal properties such as the specific heat, coefficients of thermal expansion, and thermal conductivity becomes important for such applications. In this paper, we focus on developing a model to predict effective thermal conductivity and associated local temperature and heat flux distribution within the heterogeneous materials.

The effective thermal conductivity of composites is strongly affected by many parameters including the properties, volume fractions, distributions, and orientations of constituents. Numerous models have been proposed to predict the effective thermal conductivity [Progelhof et al. 1976]. These models include simple rules of mixtures, self consistent scheme [Hashin 1968], generalized self consistent scheme [Lee et al. 2006], finite element method [Ramani and Vaidyanathan 1995; Islam and Pramila 1999; Xu and Yagi 2004; Kumlutas and Tavman 2006], effective unit cell approach [Ganapathy et al. 2005] and variational bounds [Hashin and Shtrikman 1962]. Very recently, a new framework for micromechanics modeling, namely variational asymptotic method for unit cell homogenization (VAMUCH) [Yu and Tang 2007a], has been introduced using two essential assumptions in the context of micromechanics for composites with an identifiable unit cell.

Keywords: homogenization, heterogeneous, conductivity, variational asymptotic.
This study is supported by the National Science Foundation under Grant DMI-0522908.

Assumption 1. The exact field variable has volume average over the unit cell. For example, if ϕ is the exact temperature within the unit cell, there exist ψ such that

$$\psi = \frac{1}{\Omega}\int_{\Omega} \phi \, \mathrm{d}\Omega \equiv \langle \phi \rangle, \tag{1}$$

where Ω denotes the domain occupied by the unit cell and its volume, and symbol $\equiv$ denotes a definition.

Assumption 2. The effective material properties obtained from the micromechanical analysis of the unit cell are independent of the geometry, boundary conditions, and loading conditions of the macroscopic structure, which means that effective properties are assumed to be the intrinsic properties of the material when viewed macroscopically.

Note that these assumptions are not restrictive. The mathematical meaning of the first assumption is that the exact solutions of the field are integrable over the domain of the unit cell, which is true almost all the time. The second assumption implies that we will neglect the size effects of the material properties in the macroscopic analysis, which is an assumption often made in the conventional continuum mechanics. Of course, the micromechanical analysis of the unit cell is only needed and appropriate if $\eta = h/l \ll 1$, with h as the characteristic size of the unit cell and l as the macroscopic size of the macroscopic material.

This new approach to micromechanical modeling has been successfully applied to predict thermomechanical properties including elastic properties, coefficients of thermal expansion, and specific heats [Yu and Tang 2007a; 2007b]. In this work, we will use this approach to construct micromechanics models for effective thermal conductivity and the corresponding local fields such as temperature and heat flux within a unit cell.

2. Theoretical formulation

VAMUCH formulation uses three coordinates systems: two Cartesian coordinates $\mathbf{x} = (x_1, x_2, x_3)$ and $\mathbf{y} = (y_1, y_2, y_3)$, and an integer-valued coordinate $\mathbf{n} = (n_1, n_2, n_3)$ (see Figure 1). We use x_i as the global coordinates to describe the macroscopic structure and y_i parallel to x_i as the local coordinates to describe the unit cell (Here and throughout the paper, Latin indices assume 1, 2, and 3 and repeated indices are summed over their range except where explicitly indicated). We choose the origin of the local coordinates y_i to be the geometric center of unit cell. For example, if the unit cell is a cube with edge lengths d_i, then $y_i \in [-\frac{d_i}{2}, \frac{d_i}{2}]$. To uniquely locate a unit cell in the heterogeneous material we also introduce integer coordinates n_i. The integer coordinates are related to the global coordinates in such a way that $n_i = x_i/d_i$ (no summation over i). It is emphasized that although only a square array is sketched in Figure 1, the present theory has not such limitations.

As implied by Assumption 2, we can obtain the same effective properties from an imaginary, unbounded, and unloaded heterogeneous material with the same microstrucutre as the real, loaded, and bounded one. Hence we could derive the micromechanics model from an imaginary, unloaded, heterogeneous material which completely occupies the three-dimensional space $\mathcal{R}$ and composes infinitely many repeating unit cells. The solution to the steady-state conduction problem, which is sufficient for us to find the effective thermal conductivity, can be obtained by the stationary value problem of summation of

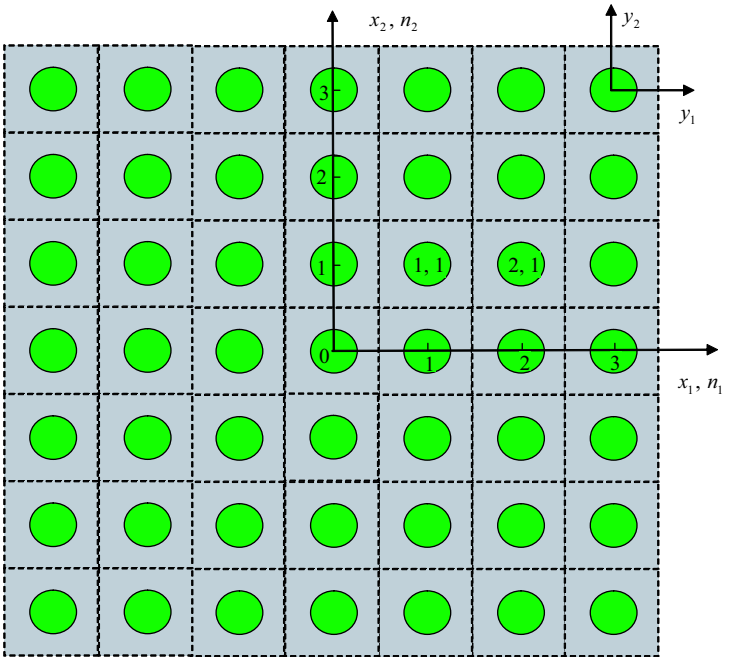

Figure 1. Coordinate systems for heterogenous materials (only a two-dimensional square array unit cell is drawn for clarity).

the "energy" integral over all the unit cells [Hashin 1968; Berdichevsky 1977], which is:

$$\Pi = \sum_{n=-\infty}^{\infty} \frac{1}{2} \int_{\Omega} K_{ij}\, \phi_{,i}\, \phi_{,j} \mathrm{d}\Omega, \tag{2}$$

where K_{ij} are components of the second-order thermal conductivity tensor, and

$$\phi_{,i}(\mathbf{n}; \mathbf{y}) = \frac{\partial \phi(\mathbf{n}; \mathbf{y})}{\partial y_i}, \tag{3}$$

with $()_{,i} \equiv \frac{\partial ()}{\partial y_i}$. Here ϕ is a function of the integer coordinates and the local coordinates for each unit cell. In view of the fact that the infinitely many unit cells form a continuous heterogeneous material, we need to enforce the continuity of the temperature field ϕ on the interface between adjacent unit cells, which is (n_1, n_2, n_3):

$$\begin{aligned}
\phi(n_1, n_2, n_3; d_1/2, y_2, y_3) &= \phi(n_1 + 1, n_2, n_3; -d_1/2, y_2, y_3), \\
\phi(n_1, n_2, n_3; y_1, d_2/2, y_3) &= \phi(n_1, n_2 + 1, n_3; y_1, -d_2/2, y_3), \\
\phi(n_1, n_2, n_3; y_1, y_2, d_3/2) &= \phi(n_1, n_2, n_3 + 1; y_1, y_2, -d_3/2).
\end{aligned} \tag{4}$$

The exact solution of the steady heat conduction problem will minimize the summation of the "energy" integral in Equation (2) under the constraints in Equations (1), and (4). To avoid the difficulty associated with discrete integer arguments, we can reformulate the problem, including Equations (2), (3), and (4),

in terms of continuous functions using the idea of the quasicontinuum [Kunin 1982]. The corresponding formulas are:

$$\Pi = \tfrac{1}{2}\int_{\mathscr{R}} \langle K_{ij}\,\phi_{,i}\,\phi_{,j}\rangle \mathrm{d}\mathscr{R}, \qquad \phi_{,i}(\mathbf{x};\mathbf{y}) = \frac{\partial \phi(\mathbf{x};\mathbf{y})}{\partial y_i}, \tag{5}$$

and

$$\begin{aligned}
&\phi(x_1, x_2, x_3; d_1/2, y_2, y_3) = \phi(x_1 + d_1, x_2, x_3; -d_1/2, y_2, y_3),\\
&\phi(x_1, x_2, x_3; y_1, d_2/2, y_3) = \phi(x_1, x_2 + d_2, x_3; y_1, -d_2/2, y_3),\\
&\phi(x_1, x_2, x_3; y_1, y_2, d_3/2) = \phi(x_1, x_2, x_3 + d_3; y_1, y_2, -d_3/2).
\end{aligned} \tag{6}$$

Using the technique of Lagrange multipliers, we can pose the thermal conduction problem as a stationary value problem for the following functional:

$$\begin{aligned}
J = \int_{\mathscr{R}} \Bigg\{ &\langle \tfrac{1}{2} K_{ij}\,\phi_{,i}\,\phi_{,j}\rangle + \lambda(\langle\phi\rangle - \psi)\\
&+ \int_{S_1} \gamma_1 \left[\phi(x_1, x_2, x_3; d_1/2, y_2, y_3) - \phi(x_1 + d_1, x_2, x_3; -d_1/2, y_2, y_3)\right] \mathrm{d}S_1\\
&+ \int_{S_2} \gamma_2 \left[\phi(x_1, x_2, x_3; y_1, d_2/2, y_3) - \phi(x_1, x_2 + d_2, x_3; y_1, -d_2/2, y_3)\right] \mathrm{d}S_2\\
&+ \int_{S_3} \gamma_3 \left[\phi(x_1, x_2, x_3; y_1, y_2, d_3/2) - \phi(x_1, x_2, x_3 + d_3; y_1, y_2, -d_3/2)\right] \mathrm{d}S_3 \Bigg\} \mathrm{d}\mathscr{R},
\end{aligned} \tag{7}$$

where λ and γ_i are Lagrange multipliers introduced to enforce the constraints in Equations (1) and (6), respectively, and S_i are the surfaces with $n_i = 1$. The main objective of micromechanics is to find the real temperature field ϕ in terms of ψ, which is a very difficult problem because we have to solve this stationary problem for each point in the global system x_i as in Equation (7). It will be desirable if we can formulate the variational statement posed over a single unit cell only. In view of Equation (1), it is natural to express the exact solution ϕ as a sum of the volume average ψ plus the difference, such that

$$\phi(\mathbf{x};\mathbf{y}) = \psi(\mathbf{x}) + w(\mathbf{x};\mathbf{y}), \tag{8}$$

where $\langle w\rangle = 0$ according to Equation (1). The very reason that the heterogenous material can be homogenized leads us to believe that w should be asymptotically smaller than ψ, that is, $w \sim \eta\,\psi$. Substituting Equation (8) into Equation (7) and making use of Equation (5), we can obtain the leading terms of the functional according to the variational asymptotic method [Berdichevsky 1977] as:

$$\begin{aligned}
J_1 = \int_{\mathscr{R}} \Bigg\{ &\langle \tfrac{1}{2} K_{ij}\,w_{,i}\,w_{,j}\rangle + \lambda\langle w\rangle + \int_{S_1} \gamma_1 \left[w(\mathbf{x}; d_1/2, y_2, y_3) - w(\mathbf{x}; -d_1/2, y_2, y_3) - \psi_{;1} d_1\right] \mathrm{d}S_1\\
&+ \int_{S_2} \gamma_2 \left[w(\mathbf{x}; y_1, d_2/2, y_3) - w(\mathbf{x}; y_1, -d_2/2, y_3) - \psi_{;2} d_2\right] \mathrm{d}S_2\\
&+ \int_{S_3} \gamma_3 \left[w(\mathbf{x}; y_1, y_2, d_3/2) - w(\mathbf{x}; y_1, y_2, -d_3/2) - \psi_{;3} d_3\right] \mathrm{d}S_3 \Bigg\} \mathrm{d}\mathscr{R},
\end{aligned} \tag{9}$$

where $()_{;i} \equiv \frac{\partial()}{\partial x_i}$. Although it is possible to carry out the variation of J_1 and find the Euler–Lagrange equations and associated boundary conditions for w, which results in inhomogeneous boundary conditions, it is more convenient to use a change of variables to reformulate the same problem so that the boundary conditions are homogeneous. Considering the last three terms in Equation (9), we use the following change of variables to express w as:

$$w(\mathbf{x};\mathbf{y}) = y_i\psi_{;i} + \zeta(\mathbf{x};\mathbf{y}), \tag{10}$$

with ζ normally termed as fluctuation functions. We are free to choose the origin of the local coordinate system to be the center of the unit cell, which implies the following constraints on ζ:

$$\langle\zeta\rangle = 0. \tag{11}$$

Substituting Equation (10) into Equation (9), we obtain a stationary value problem defined on the unit cell for ζ, such that

$$J_\Omega = \tfrac{1}{2}\langle K_{ij}\left(\psi_{;i}+\zeta_{,i}\right)\left(\psi_{;j}+\zeta_{,j}\right)\rangle + \lambda\langle\zeta\rangle + \int_{S_1}\gamma_1(\zeta^{+1}-\zeta^{-1})\mathrm{d}S_1 + \int_{S_2}\gamma_2(\zeta^{+2}-\zeta^{-2})\mathrm{d}S_2 + \int_{S_3}\gamma_3(\zeta^{+3}-\zeta^{-3})\mathrm{d}S_3, \tag{12}$$

with $\zeta^{+i} = \zeta|_{y_i=d_i/2}$, and $\zeta^{-i} = \zeta|_{y_i=-d_i/2}$, for $i = 1, 2, 3$ where $\psi_{;i}$ will be shown later to be the components of the global temperature gradient vector for the effective material with homogenized material properties. The functional J_Ω in Equation (12) forms the backbone of the present theory. This stationary problem can be solved analytically for very simple cases such as binary composites, however, for general cases we need to use numerical techniques such as the finite element method to seek numerical solutions.

3. An illustrative example

To illustrate the solution procedure of the stationary problem of the functional in Equation (12), we will consider a periodic binary composite made of anisotropic layers with material axes that are the same as the global coordinates x_i, so that the material is uniform in the $x_1 - x_2$ plane and periodic along the x_3 direction. A typical unit cell can be identified as shown in Figure 2, with the dimension along y_3 given by h and dimensions along y_1 and y_2 arbitrary. Let ϕ_1 and ϕ_2 denote the volume fraction of the first and second layer, respectively, and we have $\phi_1 + \phi_2 = 1$.

Because of the uniformity of the structure in the $x_1 - x_2$ plane, we know that the solution to ζ will be independent of y_1 and y_2, and is a function of y_3 only. Taking advantage of the this fact, we can specialize the functional in Equation (12) for this particular case in a matrix form as:

$$J^*_\Omega = \int_{S_3}\left\{\int_{-\frac{h}{2}}^{(\phi_1-\frac{1}{2})h}\left[\frac{1}{2}\Psi^{(1)T}K^{(1)}\Psi^{(1)} + \lambda\zeta^{(1)}\right]\mathrm{d}y_3 + \int_{(\phi_1-\frac{1}{2})h}^{\frac{h}{2}}\left[\frac{1}{2}\Psi^{(2)T}K^{(2)}\Psi^{(2)} + \lambda\zeta^{(2)}\right]\mathrm{d}y_3 + \gamma_3\left[\zeta^{(2)}(\frac{h}{2}) - \zeta^{(1)}(-\frac{h}{2})\right]\right\}\mathrm{d}S, \tag{13}$$

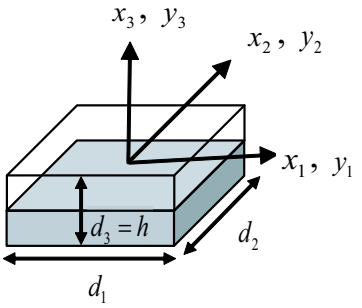

Figure 2. Sketch of a binary composite.

with $\Psi^{(\alpha)} = \lfloor \psi_{;1}\ \psi_{;2}\ \psi_{;3} + \zeta^{(\alpha)}_{,3} \rfloor^T$ for $\alpha = 1, 2$, and $\zeta^{(\alpha)}$ as the fluctuation functions of the temperature for each layer. The thermal conductivity matrix $K^{(\alpha)}$ is a fully populated symmetric matrix for a general anisotropic material, such that

$$K^{(\alpha)} = \begin{bmatrix} K^{(\alpha)}_{11} & K^{(\alpha)}_{12} & K^{(\alpha)}_{13} \\ K^{(\alpha)}_{12} & K^{(\alpha)}_{22} & K^{(\alpha)}_{23} \\ K^{(\alpha)}_{13} & K^{(\alpha)}_{23} & K^{(\alpha)}_{33} \end{bmatrix}.$$

The corresponding differential statement of the variational statement in Equation (13) can be obtained following normal procedures of the calculus of variations, as follows:

$$K^{(\alpha)}_{33}\zeta^{(\alpha)}_{,33} = \lambda, \tag{14}$$

$$\int_{-\frac{h}{2}}^{(\phi_1-\frac{1}{2})h} \zeta^{(1)}\,\mathrm{d}y_3 + \int_{(\frac{1}{2}-\phi_2)h}^{\frac{h}{2}} \zeta^{(2)}\,\mathrm{d}y_3 = 0,$$

$$\zeta^{(1)}(-\frac{h}{2}) = \zeta^{(2)}(\frac{h}{2}),$$

$$\zeta^{(1)}(\phi_1 h - h/2) = \zeta^{(2)}(\phi_1 h - h/2),$$

$$K^{(1)}_{13}\psi_{;1} + K^{(1)}_{23}\psi_{;2} + K^{(1)}_{33}\left[\psi_{;3} + \zeta^{(1)}_{,3}\right]|_{y_3=-\frac{h}{2}} = K^{(2)}_{13}\psi_{;1} + K^{(2)}_{23}\psi_{;2} + K^{(2)}_{33}\left[\psi_{;3} + \zeta^{(2)}_{,3}\right]|_{y_3=\frac{h}{2}},$$

$$K^{(1)}_{13}\psi_{;1} + K^{(1)}_{23}\psi_{;2} + K^{(1)}_{33}\left[\psi_{;3} + \zeta^{(1)}_{,3}\right]|_{y_3=(\phi_1-\frac{1}{2})h} = K^{(2)}_{13}\psi_{;1} + K^{(2)}_{23}\psi_{;2} + K^{(2)}_{33}\left[\psi_{;3} + \zeta^{(2)}_{,3}\right]|_{y_3=(\phi_1-\frac{1}{2})h}.$$

Clearly this differential statement contains two second-order ordinary differential equations in Equation (14) and five constraints for solving $\zeta^{(\alpha)}$ and λ. The solution to λ is found to be zero and $\zeta^{(\alpha)}$ are linear functions of y_3. Having solved the fluctuation functions, $\zeta^{(\alpha)}$, the density of the "energy" integral of this effective material can be trivially obtained as:

$$\Pi_\Omega = \frac{1}{2}\begin{Bmatrix} \psi_{;1} \\ \psi_{;2} \\ \psi_{;3} \end{Bmatrix}^T \begin{bmatrix} K^*_{11} & K^*_{12} & K^*_{13} \\ K^*_{12} & K^*_{22} & K^*_{23} \\ K^*_{13} & K^*_{23} & K^*_{33} \end{bmatrix} \begin{Bmatrix} \psi_{;1} \\ \psi_{;2} \\ \psi_{;3} \end{Bmatrix},$$

with the effective thermal conductivity coefficients K^*_{ij} as

$$K^*_{11} = \langle K_{11} \rangle - \frac{(K^{(1)}_{13} - K^{(2)}_{13})^2 \phi_1 \phi_2}{K^{(2)}_{33}\phi_1 + K^{(1)}_{33}\phi_2},$$

$$K^*_{22} = \langle K_{22} \rangle - \frac{(K^{(1)}_{23} - K^{(2)}_{23})^2 \phi_1 \phi_2}{K^{(2)}_{33}\phi_1 + K^{(1)}_{33}\phi_2},$$

$$K^*_{33} = \frac{K^{(1)}_{33} K^{(2)}_{33}}{\phi_2 K^{(1)}_{33} + \phi_1 K^{(2)}_{33}},$$

$$K^*_{12} = \langle K_{12} \rangle - \frac{(K^{(1)}_{13} - K^{(2)}_{13})(K^{(1)}_{23} - K^{(2)}_{23})\phi_1 \phi_2}{\phi_2 K^{(1)}_{33} + \phi_1 K^{(2)}_{33}},$$

$$K^*_{13} = \frac{K^{(1)}_{13} K^{(2)}_{33}\phi_1 + K^{(2)}_{13} K^{(1)}_{33}\phi_2}{\phi_2 K^{(1)}_{33} + \phi_1 K^{(2)}_{33}},$$

$$K^*_{23} = \frac{K^{(1)}_{23} K^{(2)}_{33}\phi_1 + K^{(2)}_{23} K^{(1)}_{33}\phi_2}{\phi_2 K^{(1)}_{33} + \phi_1 K^{(2)}_{33}}.$$

It is interesting to note that K^*_{33} is the same as the rule of mixtures based on Reuss' hypothesis for this special case. If $K^{(1)}_{13} = K^{(2)}_{13}$ and $K^{(1)}_{23} = K^{(2)}_{23}$, then K^*_{11}, K^*_{22}, and K^*_{12} are the same as the rule of mixtures based on Voigt's hypothesis, and K^*_{13} and K^*_{23} are the same as the constituent properties.

4. Finite element implementation

For more general cases, we need to rely on numerical solutions. Here, we will implement the variational statement in Equation (12) using the well-established finite element method. It is possible to formulate the finite element method solution based on Equation (12), however, it is not the most convenient and efficient way because Lagrange multipliers will increase the number of unknowns. To this end, we can reformulate the variational statement in Equation (12) as the stationary value of the following functional

$$\Pi_\Omega = \frac{1}{2\Omega} \int_\Omega K_{ij} \left(\psi_{;i} + \zeta_{,i}\right) \left(\psi_{;j} + \zeta_{,j}\right) \mathrm{d}\Omega, \tag{15}$$

under the following three constraints

$$\zeta^{+i} = \zeta^{-i}, \qquad \text{for } i = 1, 2, 3. \tag{16}$$

The constraint in Equation (11) does not affect the minimum value of Π_Ω but helps uniquely determine ζ. In practice, we can constrain the fluctuation function at an arbitrary node to be zero and later use this constraint to recover the unique fluctuation function. It is fine to use the penalty function method to introduce the constraints in Equation (16). However, this method introduces additional approximation and the robustness of the solution depends on the choice of large penalty numbers. Here, we choose to make the nodes on the positive boundary surface, $y_i = d_i/2$, slave to the nodes on the opposite negative

boundary surface, $y_i = -d_i/2$. By assembling all the independent active degrees of freedom, we can implicitly and exactly incorporate the constraints in Equation (16). In this way, we also reduce the total number of unknowns in the linear system which will be formulated as follows.

Introduce the following matrix notations

$$\Phi = \lfloor \psi_{;1}\ \psi_{;2}\ \psi_{;3} \rfloor^T, \tag{17}$$

$$\Phi_1 = \begin{Bmatrix} \frac{\partial \zeta}{\partial y_1} \\ \frac{\partial \zeta}{\partial y_2} \\ \frac{\partial \zeta}{\partial y_3} \end{Bmatrix} = \begin{Bmatrix} \frac{\partial}{\partial y_1} \\ \frac{\partial}{\partial y_2} \\ \frac{\partial}{\partial y_3} \end{Bmatrix} \zeta \equiv \Gamma_h \zeta, \tag{18}$$

where Γ_h is an operator matrix. If we discretize ζ using the finite elements as

$$\zeta(x_i;\, y_i) = G(y_i)\xi(x_i), \tag{19}$$

where G representing the shape functions and ξ a column matrix of the nodal values of the fluctuation function. Substituting Equations (17), (18), and (19) into Equation (15), we obtain a discretized version of the functional,

$$\Pi_\Omega = \frac{1}{2\Omega}(\xi^T F \xi + 2\xi^T K_{h\Phi}\Phi + \Phi^T K_{\Phi\Phi}\Phi), \tag{20}$$

where

$$F = \int_\Omega (\Gamma_h G)^T K (\Gamma_h G) \mathrm{d}\Omega, \qquad K_{h\Phi} = \int_\Omega (\Gamma_h G)^T K \mathrm{d}\Omega, \qquad K_{\Phi\Phi} = \int_\Omega K \mathrm{d}\Omega,$$

with K as the 3×3 matrix of K_{ij}. Minimizing Π_Ω in Equation (20), we obtain the following linear system

$$F\xi = -K_{h\Phi}\Phi. \tag{21}$$

It is clear from Equation (21) that the fluctuation function, ξ, is linearly proportional to Φ, which means the solution can be written symbolically as

$$\xi = \xi_0 \Phi \tag{22}$$

Substituting Equation (22) into (20), we can calculate the density of the "energy" integral of the unit cell as

$$\Pi_\Omega = \frac{1}{2\Omega}\Phi^T \left(\xi_0^T K_{h\Phi} + K_{\Phi\Phi}\right)\Phi \equiv \frac{1}{2}\Phi^T K^* \Phi. \tag{23}$$

It can be seen that K^* in Equation (23) is the effective thermal conductivity matrix, and Φ is the global temperature gradient.

If the local fields within the unit cell are of interest, we can recover those fields, including local temperature and heat flux, in terms of the macroscopic behavior, including the global temperature ψ and the corresponding gradient $\psi_{;i}$, and the fluctuation function ζ. First, we need to uniquely determine the fluctuation function. Otherwise, we could not uniquely determine the local temperature field. Because we have fixed an arbitrary node and made nodes on the positive boundary surfaces, $y_i = +d_i/2$, slave to the corresponding negative boundary surfaces, $y_i = -d_i/2$, in forming the linear system in Equation (21), we need to construct a new array $\tilde{\xi}_0$ from ξ_0 by assigning the values for slave nodes according

to the corresponding active nodes, and assigning zero to the fixed node. Clearly, $\tilde{\xi}_0$ corresponds to the stationary value of Π_Ω in Equation (15) under constraints in (16). However, $\tilde{\xi}_0$ may not satisfy (11). The real solution, denoted as $\bar{\xi}_0$, can be found trivially by adding a constant to each node so that Equation (11) is satisfied.

After having determined the fluctuation functions uniquely, we can recover the local temperature using Equations (8) and (10) as $\phi = \psi + y_i\psi_{;i} + \bar{G}\bar{\xi}_0\Phi$, where $\bar{G}$ is different from G due to the recovery of slave nodes and the constrained node. The local temperature gradient field can be recovered using Equations (3) and (18):

$$\lfloor \phi_{,1}\ \phi_{,2}\ \phi_{,3} \rfloor^T = \Phi + \Gamma_h \bar{G}\bar{\xi}_0\Phi.$$

Finally, the local heat flux field can be recovered straightforwardly using the three-dimensional Fourier law for the constituent materials, $q_i = -K_{ij}\phi_{,j}$. We have implemented this formulation in the computer program VAMUCH. In the next section, we will use a few numerical examples to demonstrate the application and accuracy of this theory and code.

5. Numerical examples

VAMUCH provides a unified analysis for general one-, two-, or three-dimensional unit cells. First, the same code VAMUCH can be used to homogenize binary composites (modeled using one-dimensional unit cells), fiber reinforced composites (modeled using two-dimensional unit cells), and particle reinforced composites (modeled using three-dimensional unit cells). Second, VAMUCH can reproduce the results for lower-dimensional unit cells using higher-dimensional unit cells. That is, VAMUCH predicts the same results for binary composites using one-, two-, or three-dimensional unit cells, and for fiber reinforced composites using two- or three-dimensional unit cells.

In this section, several examples will be used to demonstrate the accuracy of VAMUCH for predicting the effective thermal conductivity and calculating the local heat flux field within a unit cell due to temperature gradients. To facilitate comparison with existing models in the literature, we only consider composites with isotropic constituents although the present method and code can handle general anisotropic constituents.

5.1. ***Effective thermal conductivity of fiber reinforced composites.*** The first example is a carbon fiber reinforced aluminum matrix composite. Both constituents are isotropic with thermal conductivity $K = 129\ \mathrm{W/(m \cdot K)}$ for the carbon fiber, and $K = 237\ \mathrm{W/(m \cdot K)}$ for aluminum matrix. The fiber is of circular shape and arranged in a square array. The prediction of VAMUCH for the effective thermal conductivity along the fiber direction exactly obeys the rule of mixtures, which has been generally accepted as the exact solution for the longitudinal thermal conductivity for fiber reinforced composites with isotropic constituents [Hashin 1968].

However, the effective thermal conductivity coefficients in the transverse directions (K^*_{22} and K^*_{33}) do not in general obey the rule of mixtures. To validate the present theory, we compare the VAMUCH prediction with other models in the literature [Springer and Tsai 1967; Behrens 1968; Donea 1972; Hashin 1983; Hatta and Taya 1986]. As shown in Figure 3, VAMUCH results are perfectly located between the variational bounds of [Donea 1972], while the Springer–Tsai model [Springer and Tsai 1967] and the lower bound of [Hashin 1983] underpredict the results. We have also found out that

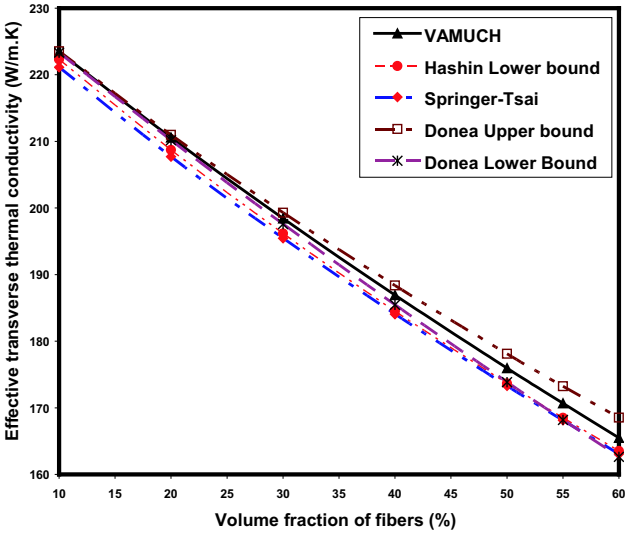

Figure 3. Effective transverse thermal conductivity of the carbon/Al composite.

VAMUCH results are the same as those obtained by Behrens [1968], Hatta and Taya [1986], and the upper bound of [Hashin 1983], and these results are not shown in the plot for clarity.

The second example is a boron fiber reinforced aluminum composite with isotropic constituents and thermal conductivity $K = 27.4$ W/(m $\cdot$ K) for the boron fiber, and $K = 237$ W/(m $\cdot$ K) for the aluminum matrix. The fiber is also circular and arranged in a square array. The effective thermal conductivities computed by different models are plotted in Figure 4. We found out that the results of the Hashin upper

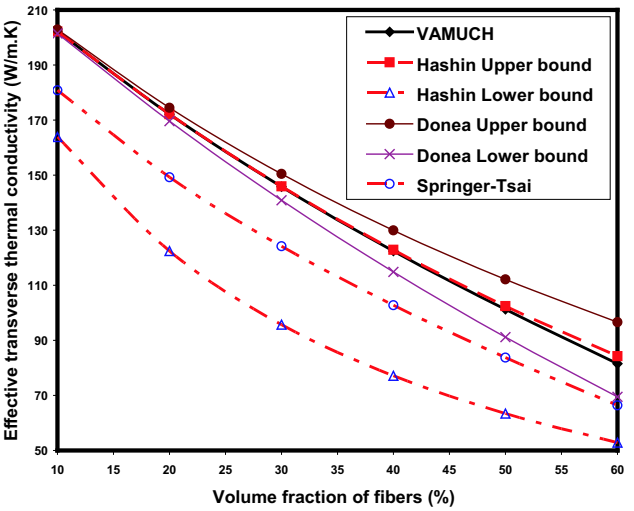

Figure 4. Effective transverse thermal conductivity of the boron/Al composite.

bound [Hashin 1983] are the same as those of [Behrens 1968] and [Hatta and Taya 1986]. Hence only the Hashin upper bound is plotted in the figure. It can be observed that the predictions of the Hashin upper bound are slightly higher than those of VAMUCH when the fiber volume fraction is higher than 40%. We also observe that the difference between the Hashin upper and lower bounds [Hashin 1983] is significant for this case which means they are not very useful for composites with constituents having relatively high contrast ratio in thermal conductivity properties. VAMUCH results are also nicely located in the much narrower bounds of [Donea 1972], while the prediction of Springer and Tsai [1967] is not accurate for this case because it is significantly lower than the lower bound of [Donea 1972].

In the two examples just described, the thermal conductivity of the matrix is higher than that of the fiber. Now, let us consider a glass/polypropylene composite with thermal conductivity $K = 1.05$ W/(m·K) for the glass fiber, and $K = 0.2$ W/(m · K) for the polypropylene matrix. We plot the change of effective transverse thermal conductivity of composites with respect to volume fraction of fibers in Figure 5. Again, we find out that VAMUCH results lie between the variational bounds of [Donea 1972]. And the results of the Hashin lower bound [Behrens 1968; Hashin 1983; Hatta and Taya 1986] are identical but slightly lower than VAMUCH results when the volume fraction of fibers is higher than 40%. Similarly, as in the previous case, we can observe that Donea [1972] provides much narrower bounds than Hashin [1983] for this case.

We also use ANSYS, a commercial finite element method package, to calculate the effective thermal conductivities of these three fiber reinforced composites. According to Islam and Pramila [1999], given the direction along which we would like to evaluate the thermal conductivity, we apply isothermal conditions to the edges perpendicular to the direction we want to evaluate the thermal conductivity and apply adiabatic conditions to the edges parallel to this direction. The effective thermal conductivity is obtained as the ratio between the average heat flux and average temperature gradient. We found out that VAMUCH results are almost the same as the ANSYS results for similar discretization schemes.

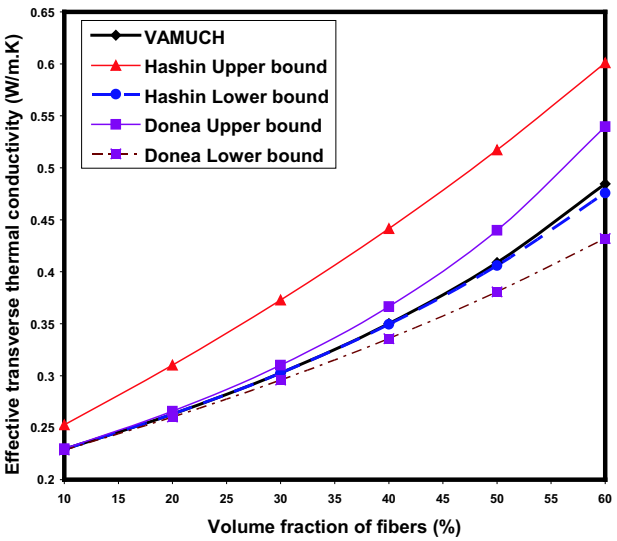

Figure 5. Effective transverse thermal conductivity of the glass/polypropylene composite.

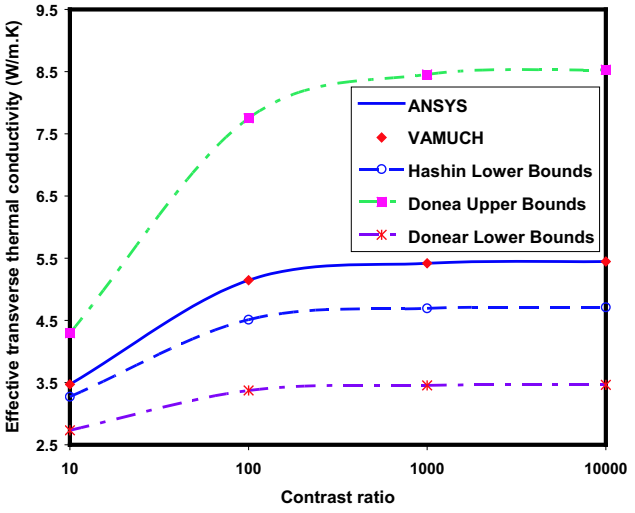

Figure 6. Effective transverse thermal conductivity with respect to varying contrast ratios.

To verify whether VAMUCH can be applied to composites with very high contrast ratio and high volume fraction, we choose a composite formed by circular fibers arranged in a square array. The volume fraction of fibers is 65%. We fix the thermal conductivity of the matrix at 1 W/(m · K), while the thermal conductivity of the fiber varies from 10 to 10^4. We plot the effective thermal conductivity computed using different approaches with different contrast ratios in Figure 6. It can be seen that VAMUCH results fall right on the curve of the ANSYS results and lie between the Donea variational bounds. The results of the Hashin lower bound [Hashin 1983] are identical to those obtained from Behrens [1968], Progelhof et al. [1976], and Hatta and Taya [1986]. It is obvious that these approaches underpredict the results. For these contrast ratios, the Hashin upper bounds are too large to be nicely plotted in the same figure.

5.2. ***Effective thermal conductivity of particle reinforced composites.*** Due to the special arrangements of the constituents of particle reinforced composites, three-dimensional unit cells are required to accurately model the microstructures. In this section, we will use VAMUCH to analyze two typical particle reinforced composites to validate the three-dimensional predictive capability of VAMUCH.

The first example is a SiC particle reinforced aluminum composite. The spherical SiC particles are embedded in a triply periodic cubic array. Both constituents are isotropic with thermal conductivities $K = 120$ W/(m · K) for the SiC particles, and $K = 237$ W/(m · K) for the aluminum matrix. The change in effective thermal conductivity of composites with respect to volume fraction of particles are plotted in Figure 7. VAMUCH results have an excellent agreement with the Hashin upper bound [Budiansky 1970; Cheng and Vachon 1970; Hashin 1983], although Budiansky [1970] and Cheng and Vachon [1970] slightly underpredict the results when the volume fraction of particles are higher than 20%. It was also found that the VAMUCH results are very close to those calculated by McPhedran and Mckenzie [1978]. All these predictions fall within the variational bounds of [Donea 1972]. It can be observed that the results

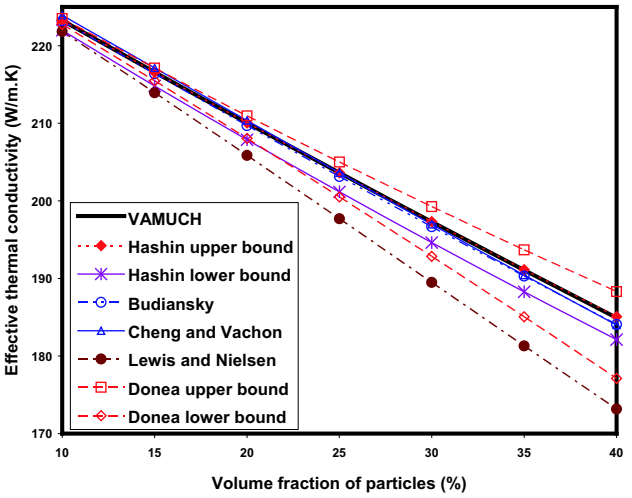

Figure 7. Effective thermal conductivity of the SiC/Al composite.

of Lewis and Nielsen [2003] significantly underpredict the effective thermal conductivity in comparison to other approaches.

Another example is an alumina (Al_2O_3) particle reinforced polyethylene composite. This composite has the same microstructure as the previous example. Both components are also isotropic with thermal conductivities $K = 31$ W/(m · K) for alumina particles, and $K = 0.545$ W/(m · K) for the polyethylene matrix. The contrast ratio of the thermal conductivity of the two components is as high as 56.88. The predictions of different approaches are shown in Figure 8. VAMUCH results agree with McPhedran and

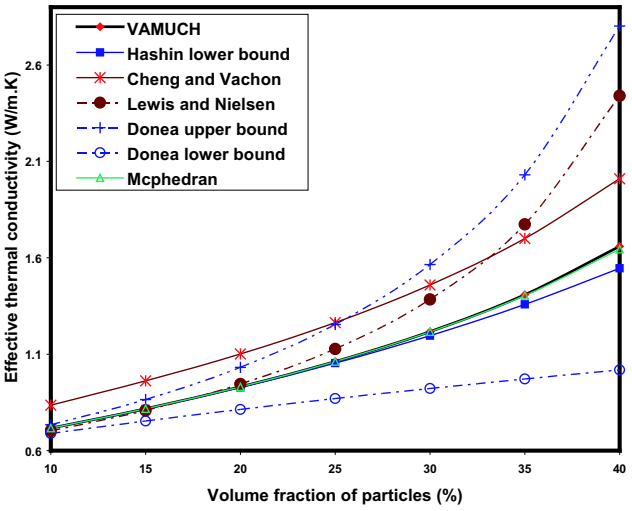

Figure 8. Effective thermal conductivity of the Al_2O_3/polyethylene composite.

Mckenzie [1978] at different volume fractions and with the lower bound of Hashin [1983] very well if the volume fraction of the particles is smaller than 25%. The prediction of Lewis and Nielsen [2003] is also very close to that of VAMUCH if the volume fraction of particles is very small. The difference between the variational bounds of [Donea 1972] becomes too large to be useful for high volume fraction of particles. The prediction of Cheng and Vachon [1970] for this case cannot be considered as accurate because it is not located between the lower and upper bounds of [Donea 1972]. We also need to point out that for this case, the results of the Hashin upper bound are too different from the lower bound and cannot be nicely plotted in the same figure.

We also analyzed these two examples of particle reinforced composites using ANSYS following the approach of Kumlutas and Tavman [2006]. Again, we found out VAMUCH results are identical to ANSYS results if similar meshes are used for both approaches.

It is noted that the Hashin bounds are known to be the best possible bounds for statistically isotropic or transversely isotropic composites, when the only available geometrical information is the phase volume fractions [Hashin and Shtrikman 1962]. However, such bounds can be improved if additional information, such as shape of inclusions and geometry of microstructure are added into the formulation [Hashin 1983]. It has been shown that the Hashin lower bound or upper bound is the exact solution for composite spheres assemblage (CSA) [Hashin 1968], which explains why one of the Hashin bounds agrees with VAMUCH very well if the inclusion volume fraction is not very large. Donea bounds [Donea 1972] are not rigorous variational bounds. Rather the material is considered as a composition of CSA within the largest possible circle/sphere and matrix. The Voigt rule of mixtures is used to obtain the Donea upper bound and the Ruess rule of mixtures is used to obtain the Donea lower bound. The effective properties of a CSA are calculated using the theory of Hashin [1968], which is also one of the Hashin bounds. Therefore, Donea bounds will fall outside at least one of the Hashin bounds, as is consistently shown in these examples. The gap between the Donea bounds could be smaller than that of the Hashin bounds because more information has been used in obtaining the Donea bounds.

5.3. ***Recovery of local heat flux.*** VAMUCH can accurately recover the local heat flux distribution within the unit cell due to temperature gradients. We will use the ANSYS results as benchmarks to verify the prediction of VAMUCH. First, we consider the glass/polypropylene fiber reinforced composite with a fiber volume fraction of 0.2. Due to the difference in thermal conductivities of the two components, the local heat flux distribution resulting from 100 K/m in the y_2 direction is not uniform within a unit cell. The distribution contours of q_2 and q_3 are plotted in Figure 9 (left and right, respectively). The sudden changes of local heat flux at the interface between the fibers and the matrix are well captured by VAMUCH. For a quantitative comparison, we also plot the local heat flux distribution q_2 along $y_2 = 0$ predicted by VAMUCH and ANSYS in Figure 10. It can be seen that there is excellent agreement between these two sets of results.

Second, we choose a special example that is a composite having an X-shape microstructure. The local heat flux distribution predicted by VAMUCH is shown in Figure 11. There are narrow necks at the corner contacts between the reinforcements that exhibit significant fluctuation in the local heat flux. The local heat flux distributions along the diagonal line predicted by VAMUCH and ANSYS are plotted in Figure 12. Excellent match between these two approaches is clear from this plot.

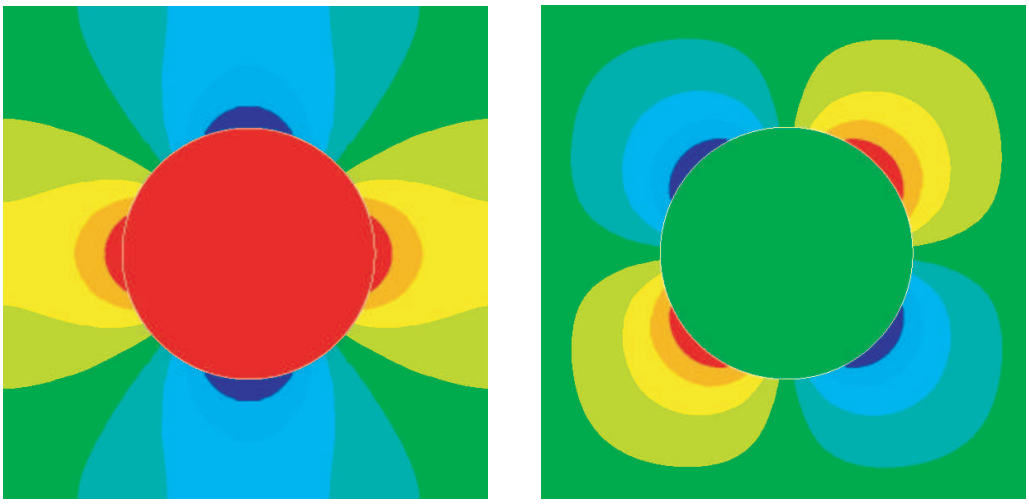

Figure 9. Left: Contour plot of heat flux q_2 in the glass/polypropylene composite. Right: Contour plot of heat flux q_3 in the glass/polypropylene composite.

6. Conclusion

The variational asymptotic method for unit cell homogenization (VAMUCH) has been extended to predict the effective thermal conductivity coefficients of composites. In comparison to existing models, the present theory has the following unique features:

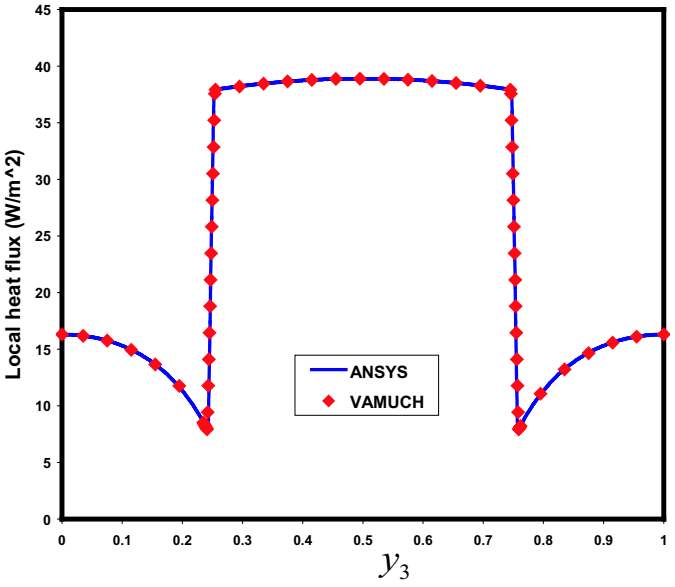

Figure 10. Heat flux q_2 distribution along $y_2 = 0$ in the glass/polypropylene composite.

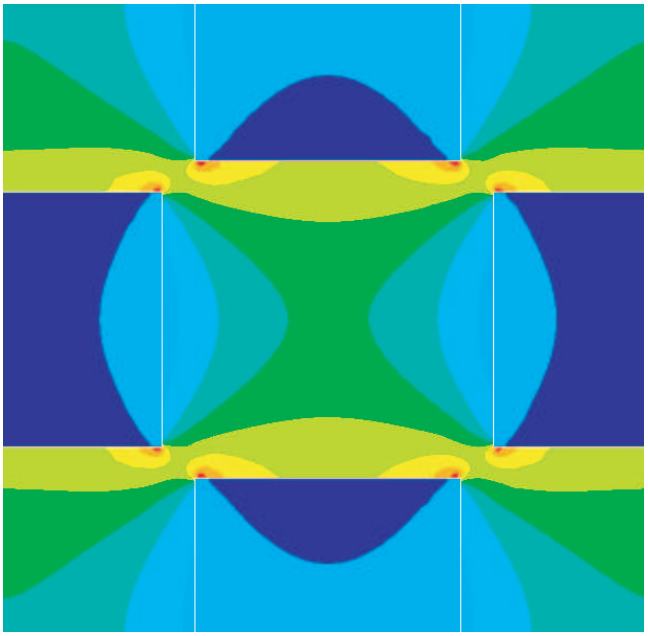

Figure 11. Contour plot of the heat flux of an X-shape composite.

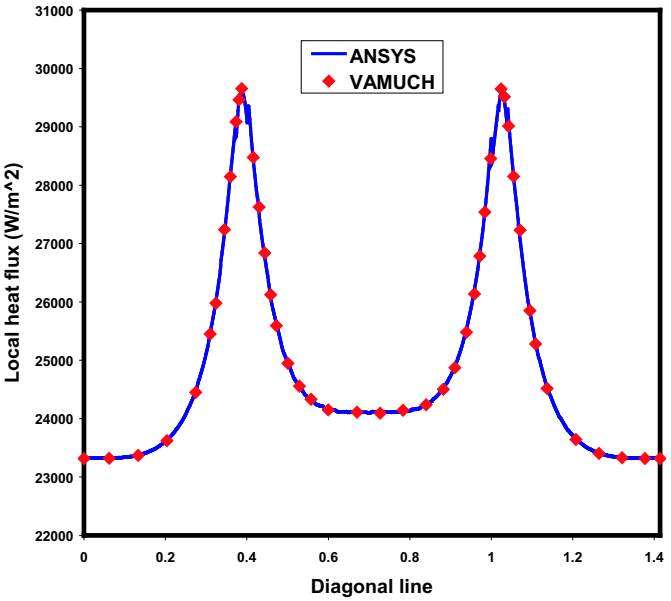

Figure 12. Heat flux of the X-shape composite along the diagonal line.

(i) It adopts the variational asymptotic method as its mathematical foundation. It invokes only essential assumptions inherent to the concept of micromechanics.

(ii) It has an inherent variational nature and its numerical implementation is shown to be straightforward.

(iii) It handles one-, two-, and three-dimensional unit cells uniformly. The dimensionality of the problem is determined by the periodicity of the unit cell.

The present theory is implemented in the computer program, VAMUCH. Numerous examples have clearly demonstrated its application and accuracy as a general-purpose micromechanical analysis tool. For the examples we have studied, although VAMUCH results are almost identical to ANSYS results, VAMUCH has the following advantages over ANSYS for micromechanical analysis:

(i) VAMUCH can obtain different material properties in different directions simultaneously, which is more efficient than those approaches requiring multiple runs under different temperature conditions.

(ii) VAMUCH can model general anisotropic heterogeneous materials with constituents having full anisotropy (with six material constants for thermal conductivity), while ANSYS and other finite element method packages can only handle constituents up to orthotropic material (with three material constants for thermal conductivity). The current finite element method approaches for predicting thermal conductivity [Islam and Pramila 1999; Kumlutas and Tavman 2006] are restricted to be at most macroscopically orthotropic, which is an unnecessary restriction.

(iii) VAMUCH calculates effective properties and local fields directly with the same accuracy as the fluctuation functions. No postprocessing calculations which introduces more approximations, such as averaging temperature gradient and heat flux, are needed.

As a byproduct of validating VAMUCH, we also provided a brief assessment of existing models for predicting effective thermal conductivity.

Due to the mathematical analogy of heat conduction, electrostatics, magnetostatics, and diffusion, the present theory and the companion code can also be used to predict effective dielectric, magnetic, and diffusion properties of heterogeneous materials.

References

[Behrens 1968] E. Behrens, "Thermal Conductivities of Composite Materials", *Journal of Composite Materials* **2** (1968), 2–17.

[Berdichevsky 1977] V. L. Berdichevsky, "On Averaging of Periodic Systems", *PMM* **41**:6 (1977), 993 – 1006.

[Budiansky 1970] B. Budiansky, "Thermal and Thermoelastic Properties of Isotropic Composites", *Journal of Composite Materials* **4** (1970), 286–295.

[Cheng and Vachon 1970] S. Cheng and R. Vachon, "A Technique for Predicting the Thermal Conductivity of Suspensions, Emulsions and Porous Materials", *International Journal of Heat and Mass Transfer* **13** (1970), 537–546.

[Donea 1972] J. Donea, "Thermal Conductivities Based on Variational Principles", *Journal of Composite Materials* **6** (1972), 262–266.

[Ganapathy et al. 2005] D. Ganapathy, K. Singh, P. Phelan, and R. Prasher, "An effective unit cell approach to compute the thermal conductivity of composites with cylindrical particles", *Journal of Heat Transfer* **127** (2005), 553–559.

[Hashin 1968] Z. Hashin, "Assessment of the self consistent scheme approximation: conductivity of particulate composites", *Journal of Composite Materials* **2** (1968), 284–300.

[Hashin 1983] Z. Hashin, "Analysis of Composite Materials-A Survey", *Applied Mechanics Review* **50** (1983), 481–505.

[Hashin and Shtrikman 1962] Z. Hashin and S. Shtrikman, "A variational approach to the theory of the effective magnetic permeability of multiphase materials", *Journal of Applied Physics* **33** (1962), 3125–3131.

[Hatta and Taya 1986] H. Hatta and M. Taya, "Thermal conductivity of coated filler composites", *Journal of Applied Physics* **59** (1986), 1851–1860.

[Islam and Pramila 1999] M. R. Islam and A. Pramila, "Thermal conductivity of fiber reinforced composites by the FEM", *Journal of Composite Materials* **33** (1999), 1699–1715.

[Kumlutas and Tavman 2006] D. Kumlutas and I. Tavman, "A Numerical and Experimental Study on Thermal Conductivity of Particle Filled Polymer Composites", *Journal of Thermoplastic Composite Materials* **19** (2006), 441–455.

[Kunin 1982] I. Kunin, *Theory of Elastic Media with Microstructure*, vol. 1 and 2, Springer Verlag, 1982.

[Lee et al. 2006] Y.-M. Lee, R.-B. Yang, and S.-S. Gau, "A generalized self consistent method for calculation of effective thermal conductivity of composites with interfacial contact conductance", *International Communications in Heat and Mass Transfer* **33** (2006), 142–150.

[Lewis and Nielsen 2003] T. Lewis and L. Nielsen, "Dynamic Mechanical Properties of Particulate-Filled Composites", *Journal of Applied Polymer Science* **14** (2003), 1449–1471.

[McPhedran and Mckenzie 1978] R. C. McPhedran and D. R. Mckenzie, "The conductivity of lattices of spheres I. the simple cubic lattice", *Proc. R. Soc. Lond. A* **359** (1978), 45–63.

[Progelhof et al. 1976] R. Progelhof, J. Throne, and R. Ruetsch, "Methods for predicting the thermal conductivity of composite systems: a review", *Polymer Engineering and Science* **16** (1976), 615–625.

[Ramani and Vaidyanathan 1995] K. Ramani and A. Vaidyanathan, "Finite element analysis of effective thermal conductivity of filled polymeric composites", *Journal of Composite Materials* **29** (1995), 1725–1740.

[Springer and Tsai 1967] G. Springer and S. Tsai, "Thermal conductivities of unidirectional materials", *Journal of Composite Materials* **1** (1967), 167–173.

[Xu and Yagi 2004] Y. Xu and K. Yagi, "Calculation of the thermal conductivity of randomly dispersed composites using a finite element modeling method", *Materials Transactions* **45** (2004), 2602–2605.

[Yu and Tang 2007a] W. Yu and T. Tang, "Variational asymptotic method for unit cell homogenization of periodically heterogeneous materials", *International Journal of Solids and Structures* **44**:11-12 (2007), 3738–3755.

[Yu and Tang 2007b] W. Yu and T. Tang, "A variational asymptotic micromechanics model for predicting thermoelastic properties of heterogeneous materials", *International Journal of Solids and Structures* **44**:22-23 (2007), 7510–7525.

Received 26 Jan 2007. Accepted 11 Jun 2007.

TIAN TANG: tiantang@cc.usu.edu
Department of Mechanical and Aerospace Engineering, Utah State University, Logan, Utah 80322-4130, United States

WENBIN YU: wenbin.yu@usu.edu
Department of Mechanical and Aerospace Engineering, Utah State University, Logan, Utah 80322-4130, United States